ISBN: 978-3-95450-204-2 ISSN: 2673-5350 doi:10.18429/JACoW-IBIC2019-TUPP006

TRANSVERSE EMITTANCE MEASUREMENT OF A 2.5 MeV PROTON BEAM ON LIPAc, IFMIF'S PROTOTYPE

J. Marroncle, B. Bolzon*, P. Abbon, T. Chaminade, N. Chauvin, S. Chel, J.-F. Denis, A. Gaget
CEA-Saclay, Gif-sur-Yvette, France
P. Cara, IFMIF/EVEDA Project Team, Rokkasho, Aomori, Japan
J. M. Garcia, D. Jimenez-Rey, A. Ros, V. Villamayor, CIEMAT, Madrid, Spain
H. Dzitko, D. Gex, A. Jokinen, A. Marqueta†, F4E, Garching, Germany
L. Bellan, M. Comunian, E. Fagotti, F. Grespan, A. Pisent, F. Scantamburlo, INFN, Legnaro, Italy
A. Rodriguez, ESS-Bilbao, Zamudio, Spain
T. Akagi, K. Kondo, M. Sugimoto, QST, Rokkasho, Aomori, Japan

Abstract

IFMIF (International Fusion Materials Irradiation Facility) is an accelerator-driven neutron source aiming at testing fusion reactor materials. Under the Broader Approach Agreement, a 125 mA / 9 MeV CW deuteron accelerator called LIPAc (Linear IFMIF Prototype Accelerator) is currently under installation and commissioning at Rokkasho, Japan, to validate the IFMIF accelerator. During the deuteron beam commissioning at 5 MeV which started in June 2018, the horizontal and vertical transverse emittance of a 2.5 MeV proton beam have been measured downstream of the RFQ for different machine configurations. Such measurements were done with an emittance measurement unit composed of slits defining a beamlet of 200 µm width, then of steerers and finally of a SEM-Grid monitor. In this paper, the process and the system are first described. The secondary electron emission of SEM-Grid wires is then estimated based on measurements and results are close to the usual rule of thumb. Finally, emittance measurements are presented and comparisons with beam dynamics simulations show good agreement.

INTRODUCTION

The International Fusion Materials Irradiation Facility (IFMIF) is an accelerator-driven D-Li neutron source that will produce high energy neutrons at high intensity to characterize and qualify fusion reactor materials [1-3]. It aims of accelerating 125 mA/CW deuterium ion beam (D^+) up to 40 MeV. Its design performance will step forward present accelerator technological frontiers. It is presently in its engineering validation phase [4-7] with the Linear IFMIF Prototype Accelerator (LIPAc). The LIPAc aims to validate the IFMIF accelerators up to the first SRF Linac with a 125 mA / 9 MeV CW deuteron accelerator. It is being assembled, commissioned and will be operated in Rokkasho under the Broader Approach agreement, concluded between the European Atomic Energy Community (Euratom) and the Government of Japan.

After the injector commissioning phases A and B0 [8-10] with 140 mA/100 keV D^+ beam extraction, the LIPAc commissioning is currently in its phase B. This phase consists of accelerating D^+ beam through the RFQ up to 5 MeV in pulsed mode at low duty cycle (0.1% in nominal) [11], and to transport the beam through the Medium Energy Beam Transport (MEBT) line and the Diagnostic Plate (D-Plate) up to the Low Power Beam Dump (LPBD). The commissioning of the MEBT line [12], to match the beam entrance characteristics into the SRF, and the commissioning of beam diagnostics are ongoing [13].

For a first tuning of the different subsystems, an equal perveance 70 mA/50 keV proton beam (H^+) has been successfully accelerated at the beginning of phase B (on 13th June 2018) up to 2.5 MeV through the RFQ [14]. The full characterization of the H^+ beam has been performed with a large variety of diagnostics located on the D-Plate. Among them, an emittance measurement unit (EMU) composed of slits, steerers and a SEM-Grid monitor had been set-up to allow horizontal and vertical emittance measurements without space charge issue. In this paper, the EMU is first described. Then, the beam profile measurements performed with the SEM-Grid alone are presented in order to give an estimation of secondary electron emission on wires. Finally, the emittance measurements are presented and compared to beam dynamic simulations.

EMITTANCE MEASUREMENT

Introduction

The emittance measurement in the D-Plate has to be made with 2.5 MeV H^+ beam and 5 MeV D^+ beam (D-Plate located currently downstream of the RFQ), and with 4.5 MeV H^+ beam and 9 MeV D^+ beam (D-Plate located in the future downstream of the SRF-Linac). The principle is depicted on Fig. 1 for a horizontal emittance measurement (X-axis). A short pulse length beam, coming from the left, is meanly stopped in a movable slit able to sustain high beam power deposition (aperture: 100 or 200 µm), leaving only a beamlet passing through it. The maximum pulse length is 100 µs (repetition rate of 1 Hz) assuming the nominal beam current of 125 mA. The beamlet profile is measured on the Y-SEM-Grid plane for each position of the vertical slit (Y-axis) moving transversely wrt X-axis. This method gives access to the angular divergence of the beam versus its transverse coordinate (X), from which the X-emittance is extracted.

The LIPAc's SEM-Grid monitor has large wire gaps (1, 2 and 3 mm), limiting the measurement resolution of the

* benoit.bolzon@cea.fr
† Presently at ITER, Cadarache, France.

ISBN: 978-3-95450-204-2 ISSN: 2673-5350 doi:10.18429/JACoW-IBIC2019-TUPP006

beamlet profile. To overcome this problem, electromagnetic steerers are inserted between the slit and the SEM grids. The different deviation settings are chosen in such a way that the beamlet moves on the grids, allowing different overlapping between beamlet and wires.

Note that the beam emittance measurement is done in X and Y directions, necessitating 2 Slits (X & Y), 2 steerers and X&Y wires planes.

In the following, we propose to give few characteristics of the slits and to detail the steerers.

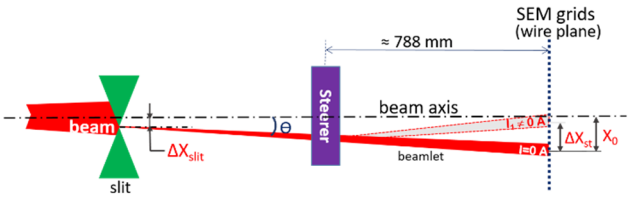

Figure 1: Beam emittance measurement principle: a short-pulsed beam at nominal conditions is stopped on a movable slit. For each slit position, the beamlet profile is measured on the SEM-Grid for several electromagnetic deviations.

The Slit

Two high power slits, vertical and horizontal, were designed and provided by CIEMAT Madrid [13]. The main characteristics are their ability to sustain the nominal deuteron beam current (125 mA) during 100 µs at 9 MeV and 1 Hz, thus 112 W, for beam sizes σ spreading over 5 to 6 mm. The aperture can be set at 100 or 200 µm after a mechanical intervention. Actuators allow the slits inserting, moving and removing, into or from the beam. Only one slit can be inserted at a time leading to the horizontal or the vertical beam emittance measurement. Deposited heat is removed with a water cooling system. All these actions are safely done, under a Programmable Logic Controller (PLC) to avoid any permanent damages and permits are delivered by MPS.

The Deviator

The deviator is made with a squared frame on which are set 2 pairs of similar coils, for lateral and vertical beamlet shift. This frame, pictured on Fig. 2-a, has an aperture greater than 105 mm, to be installed around the beam pipe. Each coil is wounded around an Armco plate with a 60 mm × 22 mm cross section. The enameled (7 µm) conductor wire has a rectangular shape (4.64 mm × 1.14 mm).

The largest $\int \vec{B} \cdot \vec{dl}$ occurred for a deuteron beam at 9 MeV, which should be above 23.3 G.m for a deviation of 3 mm at the SEM-Grid location. To achieve this value, a coil is made by 7 layers of 21 spires, feeds by an 11 A current. Tests done in the company premises (SEF[1]) confirmed this value, which is also in agreement with the Opera software used at CEA Saclay for the design. Some precaution should be taken to avoid increasing of the temperature, since the current coil left at 12 A during 8 hours increases the temperature up to 80°C.

A specific power supply was designed by VP Electronics[2] providing 2 channels (X and Y) at ±11 A and 15 V.

Finally, a magnetic shielding (blue plate in the background) with a 105 mm aperture was set downstream the steerer for minimizing the magnetic leakages which should compromise the DCCT measurements. The total length of the steerer in the beam direction is about 80 mm, while 185 mm in the transversal section. The $\int \vec{B} \cdot \vec{dl}$ was measured at Saclay for several currents and at different positions; the B field was measured at 11 A on the X-direction for various elevations as shown on Fig. 2-b. Such data will be used to simulate and unfold the several beamlets profiles in order to reconstruct the emittance from measurements.

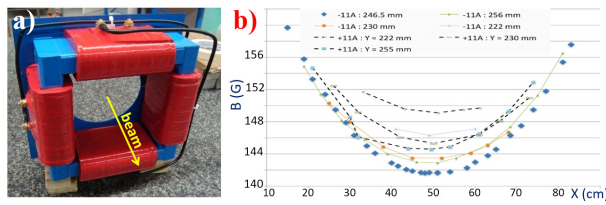

Figure 2: a) The deviator with its two coil pairs (red) wounded on the squared frame (blue) and the magnetic shielding plate on the back. b) The magnetic field measurement done with a Hall probe at 11 A along the X-axis for several probe elevations.

SEM-GRID

Description

There is one SEM-Grid implemented on the D-Plate. It was designed and manufactured by Ganil [15]. It consists of the following components:

- A vacuum part which is mounted on a CF-DN200 viewport flange fixed on the D-Plate.
- An actuator allows managing, through a PLC, the insertion and the extraction of a pair of similar wire grids, tilted by 90º for X and Y profile measurements. Each grid is made in ceramics (Rogers 4350B) squared frame with an aperture of 100 mm. Wires are alternatively soldered on both frame sides. The width covered by the wires is 86 mm distributed with 3 gaps (1, 2 and 3 mm). An extra wire surrounds the frame in order to create a loop polarized around +100 V, acting as an electron repeller.
- A front-End Electronics, integrating the secondary electron emission current through capacitors, over a time ranging from 40 µs to 16 s for the 94 active wires.

Tungsten golden plated wires of 20 µm diameter shall work with 2.5/4.5 MeV H^+ beam or 5/9 MeV D^+ beam.

Secondary Electron Emission

Despite theory [16], a well-known rule of thumb gives an estimation of the secondary electron current left generated by a charged particle impinging on a wire. It is based on the fact that only electrons released during ionization

[1] SOCIETE D'ETUDE ET DE FABRICATION pour la recherche et l'industrie, 320 rue du Chêne Vert, 31670 Labège, France.

[2] VP Electronique, 91746 Massy Cedex, France.

ISBN: 978-3-95450-204-2 ISSN: 2673-5350 doi:10.18429/JACoW-IBIC2019-TUPP006

processes in a 1 nm external layer of the wire, may have chance exiting the wire, then contributing to the SEM current. For a 2.5 MeV proton beam, the mean energy deposited by a proton in tungsten material is around 100 eV as calculated by the SRIM software [17]. Considering that 25 eV are necessary for ionizing/ejecting an electron, this leads to 4 electrons, but 2 of them are emitted toward the inner wire and therefore will be absorbed, while the 2 others can escape. If the proton energy is enough high to cross the wire when entering and escaping it, then the expected electron number should be 2+2 = 4 electrons per incident positive particle.

Measurement

During the LIPAc commissioning, profile measurements of a 2.5 MeV proton beam were performed like the depicted one on Fig. 3, which is fitted by a Gaussian. Although the measured profile is a bit far from the Gaussian shape, we take care to have the same integral for both of them. We use this fit for convenience, as it is easy to calculate the geometrical overlapping between a Gaussian beam and a wire. The result gives the ratio of 2.26 SE electrons per incident proton, whilst we expected 4! Looking on Fig. 4-a, one can see that the SRIM depth of proton into tungsten can go up to 22 µm.

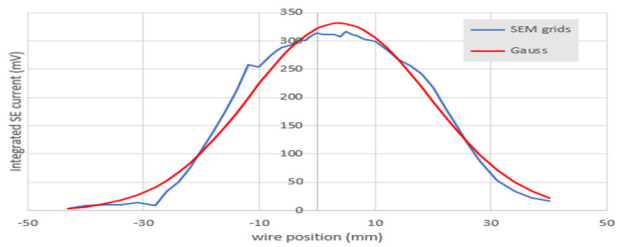

Figure 3: Beam profile measurement and its Gaussian fit.

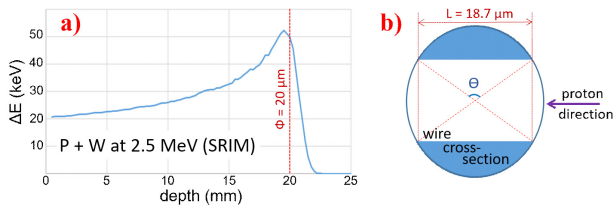

Figure 4: a) The proton range versus the depth in tungsten medium, calculated with SRIM. b) The 20 µm wire cross section with the blue part corresponding to the full crossing of proton.

Several reasons may explain this result: the rule of thumb is just an approximation using 1 nm layer thickness which should be dependent on the material, the range can be shorter than the calculated one due to nuclear reactions for instance, the diameter of the wire is not exactly 20 µm, the electron energy of 25 eV is not guaranteed when the proton is on the way to be stopped in the medium… To illustrate that, we propose to calculate the range value in order to have exactly a ratio 2.26/4. On Fig. 4-b, the geometric cross section of the wire is drawn, by assuming that only beam particles crossing the blue sections can escape the wire. The circular segment surface leads to the following relation:

$$\frac{R^2(\theta - sin\theta)}{\pi} = \frac{2.26}{4} \Rightarrow \theta = 2.43 \text{ rad and } L = 18.7 \text{ µm}$$

This value calculated with a 20 µm diameter wire is quite close to the range. We can conclude that such experimental conditions are not adequate to check the SE current by this way.

Therefore, we propose to redo the calculation with a deuteron beam at 5 MeV for which the range is of the order of 43 µm, much larger than the wire diameter.

During this summer, the profile of a 5 MeV pulsed deuteron beam of 118 mA and 200 µs width (repetition rate of 1 Hz) was measured with the SEM-Grid, for a large transverse beam size of around 17.5 mm (σ). Considering a tungsten thickness of 15.7 µm (circular to equivalent rectangular shape: πR/2), SRIM shows an energy deposit of 1.4 MeV for 5 MeV incident deuteron, leading to a mean loss energy of 89 eV/nm. Thus, the expected electron/incident deuteron should be 89/25 = 3.6. This is in good agreement with the experiment since we measured 3.3, a difference of 7%.

EMITTANCE PROCEDURE

Description

The automatic procedure for emittance measurement is described below:

- Slit displacement of ΔX_{slit} (e.g. 1 mm).
- Steerer setting at 0 A (no beam deviation)
- Data acquisition: the signal integration is performed for each pulse. The measurement is done *n* times (*n* being an input user parameter) to get correct statistics and to avoid the saturation of the integrators (capacitors of the front-End Electronics). In fact, the integrators are reset for each pulse to avoid saturation effects.
- First beamlet displacement ΔX_{st1} by applying the first steerer current I_{st1}, then acquisition of the charge for each of the *n* pulses,
- Idem for ΔX_{st2} (I_{st2}) and ΔX_{st3} (I_{st3}). The measurement for this slit position is now achieved.
- Slit displacement of ΔX_{slit}
- Etc…

Choice of the Steerer Currents

Four steerer currents (including I_{st} = 0 A) are applied in the automatic emittance measurement procedure in order to allow sufficient resolution on the beamlet profile measurement and in the same time to allow quite fast measurement. The optimum steerer currents have been calculated using the TraceWin software [18] into which the magnetic field maps of the steerers were integrated. These currents have been calculated for the four cases of LIPAc: 2.5/4.5 MeV H^+ beam and 5/9 MeV D^+ beam. They are automatically applied on the automatic emittance measurement software depending on the type and energy of particles.

ISBN: 978-3-95450-204-2 ISSN: 2673-5350 doi:10.18429/JACoW-IBIC2019-TUPP006

Emittance Measurement and Analysis

Horizontal and vertical emittance measurements have been performed on March 2019 with H^+ beam for different current settings of the two solenoids (SOL1 / SOL2) of the Low Energy Beam Transport (LEBT) line and for different settings of the RFQ voltage (V_{RFQ}). The beam current was measured with an ACCT (AC Current Transformer) and was of around 22 mA near the EMU location. The transverse beam size was measured with the SEM-Grid alone and was of 10 mm (1 σ). The maximum beam pulse length, before reaching the thermionic temperature of the SEM-Grid wires, was calculated to be of 800 µs taking into account the beam current and transverse size. This pulse length was set for the emittance measurement to maximize the signal to noise ratio (beam repetition rate of 1 Hz).

A script allowing to reconstruct automatically the emittance from experimental data files has been developed in Python language [19]. It uses internally the TraceWin software together with the magnetic field maps of the steerers for the calculation of the beamlet displacement. Since the magnetic field is not uniform in the steerers, the slit position is taken into account in the latter calculation.

As an example, the reconstructed vertical emittance from measurements performed with SOL1= 131 A, SOL2= 162 A and V_{RFQ}= 70 kV is shown on a histogram in Fig. 5-a. The angular resolution is very good, which means that a number of four steerer currents is largely enough. To calculate the emittance from this histogram, the background noise has to be subtracted. As a first analysis, intensity below a defined threshold is considered as background and is removed, see Fig. 5-b where a threshold of 10 was applied (same threshold applied in Table 1). The emittance results are quite sensitive to this threshold setting. To solve this issue, signal to noise ratio should be increased by decreasing the capacitors values of the front-End Electronics.

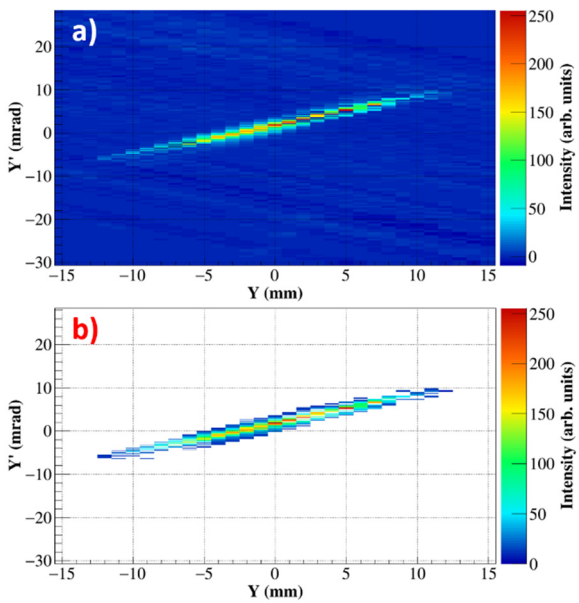

Figure 5: Emittance measurement with 2.5 MeV H^+ beam. a) Raw data. b) Background subtracted. SOL1/SOL2= 131/162 A, V_{RFQ}= 70 kV. Around EMU location: current= 22 mA, 1 σ= 10 mm, pulse length= 800 µs, repetition= 1 s.

Comparison with Simulated Beam Emittance

Beam dynamics simulations have been performed [20] [14] with the same beam parameters than the ones set for emittance measurements. Table 1 compares the results between vertical emittance measurements and simulations. For point 4, some differences exist that will be investigated in a near future with simulations and post analysis. Apart for point 4, results of the normalized emittance are in very good agreement. Small differences exist in the Twiss parameters, but the trend is completely followed. For instance, when the Twiss Parameters decrease in measurement, they do the same in simulation. However, these results should be taken as preliminary results due to the background issue that was explained previously.

Table 1: Comparison Between Measurements and Simulations of the Vertical Emittance at the D-Plate Location

Measurement	1	2	3	4
SOL1 [A]	135	135	135	131
SOL2 [A]	160	160	162	162
V_{RFQ} [kV]	66	62	70	70
Norm. ε_{exp} / ε_{sim} [π mm mrad]	0.24 / 0.24	0.24 / 0.24	0.22 / 0.23	0.24 / 0.28
β_{exp} / β_{sim} [mm/π mrad]	7.1 / 7.5	8.0 / 8.1	6.6 / 6.3	6.5 / 6.0
α_{exp} / α_{sim}	-4.8 / -5.5	-5.4 / -6.0	-4.3 / -4.3	-4.4 / -4.5

CONCLUSION

The secondary electron emission of wires of the SEM-Grid used for emittance measurement has been estimated based on beam profile measurements. Results are close to what is expected from the usual rule of thumb, which confirm our understanding on signals issued from SEM-Grids.

Preliminary comparisons between emittance measurements and simulations for different machine settings show good agreements, which validate the correct functioning of the EMU. However, signal to noise ratio should be enhanced in order to improve the accuracy of the emittance measurement. For that, cards integrating capacitors of lower values will be exchanged in the front-End Electronics during the next maintenance phase. Also, the improvement of the data analysis on background subtraction can help improving the precision on results. Finally, error bars taking into account the different systematic errors that exist on the EMU should be integrated in the data analysis.

ACKNOWLEDGEMENTS

The present work has been performed in framework of the Broader Approach (BA) Agreement. The authors gratefully acknowledge the support of their home institutions and research funders in this work. Views and opinions expressed herein do not necessarily reflect those of QST, Fusion For Energy, or of the author's home institutions or research funders.

The authors would like to thank E. Dessay and J.C. Foy from Ganil (Caen, France) for their very relevant help and valuable expertise for the SEM-Grid functioning.

ISBN: 978-3-95450-204-2 ISSN: 2673-5350 doi:10.18429/JACoW-IBIC2019-TUPP006

REFERENCES

[1] IFMIF International Team, "IFMIF Comprehensive Design Report", *IEA on-line publication*, 2004.

[2] J. Knaster et al., "IFMIF, the European–Japanese efforts under the Broader Approach agreement towards a Li(d,xn) neutron source: Current status and future options", *Nucl. Mater. Energy 9*, 2016, pp. 46-54. doi:10.1016/j.nme.2016.04.012

[3] J. Knaster, A. Moeslang, and T. Muroga, "Materials research for fusion, *Nature Physics 12,* 2016, pp. 424-434. doi:10.1038/NPHYS3735

[4] J. Knaster, et al., "Overview of the IFMIF/EVEDA project", *Nucl. Fusion 57*, 2017, 102016, 25pp. doi:10.1088/1741-4326/aa6a6a

[5] P. Garin and M. Sugimoto et al., "Main baseline of IFMIF/EVEDA project", *Fusion Eng. Des. 84,* 2009, pp. 259-264. doi:10.1016/j.fusengdes.2008.12.040

[6] R. Heidinger et al., "Progress in IFMIF EngineeringValidation and Engineering Design Activities", *Fusion Eng. Des. 88*, 2013, pp. 631-634. doi:10.1016/j.fusengdes.2013.01.066

[7] P. Cara et al., "The Linear IFMIF Prototype Accelerator (LIPAC) Design Development under the European-Japanese Collaboration", *in Proc. IPAC'16*, Busan, Korea, 2016, paper MOPOY057, pp. 985-988. doi:10.18429/JACoW-IPAC2016-MOPOY057

[8] N. Chauvin et al., "Deuteron beam commissioning of the linear IFMIF prototype accelerator ion source and low energy beam transport", *Nucl. Fusion 59,* 106001, 2019, 9pp. doi:10.1088/1741-4326/ab1c88

[9] B. Bolzon et al., "Beam diagnostics of an ECR ion source on LIPAc injector for prototype IFMIF beam accelerator", *Fusion Eng. Des. 136*, 2018, pp. 1300-1305. doi:10.1016/j.fusengdes.2018.04.128

[10] T. Akagi et al., "Commissioning of High Current H+/D+ ion beams for the Linear IFMIF Prototype Accelerator (LIPAc)", *in Proc. ICIS'19*, Lanzhou, China, 2019.

[11] K. Kondo et al., "Linear IFMIF Prototype Accelerator (LIPAc) : Installation activities for Phase-B beam commissioning in Rokkasho", *Nucl. Mat. Energy 15*, 2018, pp. 195-202. doi:10.1016/j.nme.2018.04.011

[12] I. Podadera et al., "Commissioning of the LIPAc medium energy beam transport line", *in Proc. IPAC'18*, Vancouver, BC, Canada, 2018, paper TUPAF012, pp. 683-686. doi:10.18429/JACoW-IPAC2018-TUPAF012

[13] D. Jimenez-Rey et al., "Overview of LIPAc Beam instrumentation for the initial accelerator commissioning", *in Proc. IBIC'19*, Malmo, Sweden, 2019.

[14] E. Fagotti et al., "IFMIF/EVEDA RFQ preliminary beam characterization", *in Proc. LINAC'18*, Beijing, China, 2018, paper THPO062, pp. 834-837. doi:10.18429/JACoW-LINAC2018-THPO062

[15] J.L. Vignet et al., "The beam profile monitors for SPIRAL2", *in Proc. DIPAC09*, Basel, Switzerland, 2009, paper TUPB07, pp. 176-178.

[16] E.J. Sternglass, "Theory of Secondary Electron Emission by High-Speed Ions", *The Physical Review 108(1)*, 1957, pp. 1-12.

[17] SRIM (Stopping and Range of Ions in Matter), J.F. Ziegler et al., www.srim.org

[18] D. Uriot, and N. Pichoff, "Status of Tracewin code", *in Proc. IPAC'15,* Richmond, VA, USA, 2015, paper MOPWA008, pp. 92-94. doi:10.18429/JACoW-IPAC2015-MOPWA008

[19] Python programming language, https://www.python.org

[20] L. Bellan et al., "Beam dynamics of the first beams for IFMIF-EVEDA RFQ commissioning", *in Proc. IPAC'18*, Vancouver, BC, Canada, 2018, paper THPAK019, pp. 3246-3248. doi:10.18429/JACoW-IPAC2018-THPAK019